Tripathi, Tripurari S.; Karppinen, Maarit

Experimental setup for anisotropic thermoelectric transport measurements using MPMS

Published in:
Measurement Science and Technology

DOI:
10.1088/1361-6501/aaf609

Published: 01/02/2019

Document Version
Peer-reviewed accepted author manuscript, also known as Final accepted manuscript or Post-print

Please cite the original version:
Tripathi, T. S., & Karppinen, M. (2019). Experimental setup for anisotropic thermoelectric transport measurements using MPMS. *Measurement Science and Technology*, *30*(2), Article 025602. https://doi.org/10.1088/1361-6501/aaf609

Experimental setup for anisotropic thermoelectric transport measurements using MPMS

Tripurari S Tripathi,* Maarit Karppinen*

[1] Department of Chemistry and Materials Science, Aalto University, Espoo, Finland

E-mails: tripurari.tripathi@aalto.fi; maarit.karppinen@aalto.fi

Received xxxxxx
Accepted for publication xxxxxx
Published xxxxxx

Abstract

At reduced dimensions electrical transport properties of materials often depend on the measurement direction. Here we report a measurement setup designed on the manual insertion utility probe (MIUP) of the Quantum Design's magnetic property measurement system (MPMS) to measure anisotropic transport properties in the temperature range of 10–400 K and magnetic fields up to 5 Tesla. The setup is capable of measuring Seebeck coefficient and electrical resistivity both along and perpendicular to the applied magnetic field. The Seebeck measurement is based on the differential measurement technique; the four-probe electrical resistivity measurement can easily be performed on the opposite side of the setup. The setup consists of a small copper cube (5x5x5 mm^3) fitted with diagonally cut electrically insulated square strips. The strips are fitted with copper-constantan thermocouple in differential arrangement for the temperature-gradient (ΔT) measurement and symmetrically arranged surface mount (SM) resistors to create the ΔT across the sample. The cube can be rotated to alter the direction of applied magnetic field on the sample. We demonstrate the directional dependence of the measured transport properties for a normal platinum wire and also for single crystal flakes of $CuCr_2Se_4$.

Keywords: Anisotropic electrical transport measurement, Seebeck coefficient, Electrical resistivity, MPMS

1. Introduction

Measurement of the Seebeck coefficient is of great importance in understanding the electronic transport properties of various functional materials, owing to the extreme sensitivity of it to the particle-hole asymmetry [1, 2]. For example, the ambipolarity of graphene cannot be probed by conductance measurements alone [3]. Thermoelectrics is another steadily growing field where state-of-the-art Seebeck coefficient measurements are required for both bulk and thin-film samples [4-12]. In addition, Seebeck coefficient measurements under magnetic field [13] could provide a valuable experimental tool to investigate magnetothermoelectric effects, such as the Nernst effect in two-dimensional electronic systems [14, 15], quantum phase transitions [16], and magnon drag effects [17], etc. Moreover, for low dimensional materials that show sharp changes in density of states around Fermi level Seebeck coefficient measurements in different magnetic field and temperature gradient configurations can add extra degree of freedom to the study and optimization of these materials for applications [18, 19].

In recent years, low dimensional materials have been strongly highlighted, and for several such materials promising thermoelectric properties have been reported as well, e.g. MoS_2 [20, 21], WSe_2 [22, 23], TiS_2 [24] and Na_xCoO_2 [25]. However, in only rare cases their anisotropic Seebeck properties have been measured. Thus, there is a definite need for a simple, quick, and affordable experimental setup to estimate the directional dependences of Seebeck coefficient.

There are two main techniques for Seebeck coefficient measurement, the integral and differential measurement methods; nevertheless, there are several variants of these techniques, such as scanning probe technique [26, 27], integrated heater sensor technique [28], two thermocouple or differential technique [29, 30], etc. In the integral method Seebeck coefficient is estimated from the voltage of a thermocouple system consisting of the sample and a reference electrode wire. The serious disadvantage of this method is that the sample must be longer, wires or metallic ribbons shaped, and semimetals, which is not possible always. In contrast, the differential method is designed for measuring Seebeck coefficients for short samples of any shape, including thin films. Therefore, the vast majority of Seebeck measurements are performed using this method. In this method the temperature difference between two points on the sample is measured with two thermocouples (or temperature sensors) in normal or differential configuration; the resultant Seebeck signal ΔV can be measured by the same branches of thermocouples or separate voltage probes. The recent review by Martin et al. [31] provides an overview of the challenges and various practices of high-temperature thermoelectric metrology on bulk materials.

The setup reported here is simple, inexpensive, and accurate for the Seebeck coefficient measurements of thin samples such as single crystal flakes and thin films of cumulative thickness including the substrate not greater than 1 mm, in the temperature range of 10–400 K and magnetic fields up to 5 Tesla. The maximum uncertainty in the measured thermoelectric power (TEP) is less than 0.2 μV/K, whereas the accuracy is within 4%. As shown in Figure 1, the direction of magnetic field on the sample can be altered in our setup from cross-plane to in-plane temperature gradient by rotating the cube along its axis. The same setup can also be used for electrical resistivity/magnetoresistance measurements; for these measurements the sample is mounted on face of the cube opposite to the one used in the Seebeck measurements. The setup consists of two surface mount (SM) chip resistors, two diodes, one current source, and one nanovoltmeter to both create and measure the ΔT and ΔV. A copper-constantan (type-T) thermocouple in differential geometry is used for the measurement of ΔT. The use of diodes reduces the need of number of instruments required for data acquisition. We have earlier reported a similar setup using a liquid nitrogen cryostat for zero field measurements [32]. However, the present setup has novel design that provides more versatility in measurements. With provisions to rotate the sample holder w.r.t. magnetic field and the availability of two equivalent sample mounting positions, one can explore the several permutations of magnetic field and temperature gradient directions for measurements.

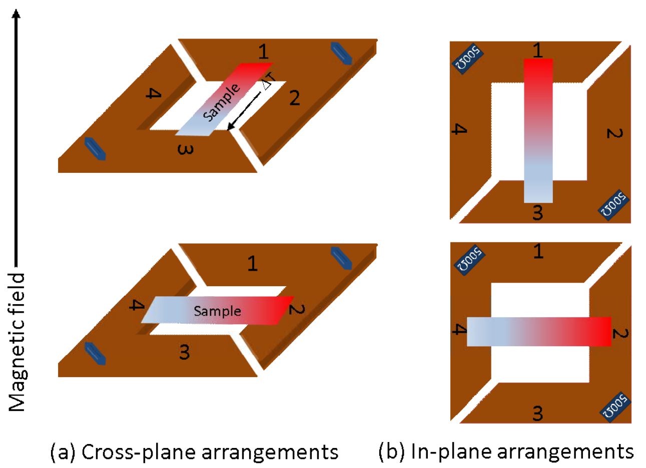

Figure 1. Different configurations of the sample with respect to magnetic field on it (a) magnetic field is perpendicular to the to the sample surface/temperature gradient (b) magnetic field is parallel to the sample surface and parallel/perpendicular to temperature gradient.

2. Experimental

The complete arrangement of the measurement setup is presented in Figure 2. It is designed on a manual insertion utility probe (MIUP; Quantum Design), see Figure 2(a). The sample mounting copper strip can be removed from the MIUP to attach the new setup for the directional measurements. A photo of the actual setup is shown in

Figure 2(b). We fabricated the setup on a brass rod 7 mm in diameter and 30 mm in length. It consists of a copper cube that can be rotated along the axis perpendicular to the direction of the applied magnetic field. Figure 2(c) displays the zoomed image of the square copper strips on cubic copper base in a bridge arrangement. The strips are electrically insulated from the copper base. The bridge consists of SM symmetrically placed on the opposite corners of the square strips to create the equivalent ΔT between points (1,3) and (2,4). A differential arrangement of copper-constantan thermocouple between points (2,4) is arranged for measurement of ΔT. A schematic image of the whole setup is shown Figure 2(d). The whole data acquisition assembly including the magnetic property measurement system (MPMS; Quantum Design MPMS 5XL SQUID Magnetometer), current source and nanovoltmeter is controlled by National Instruments LabView software.

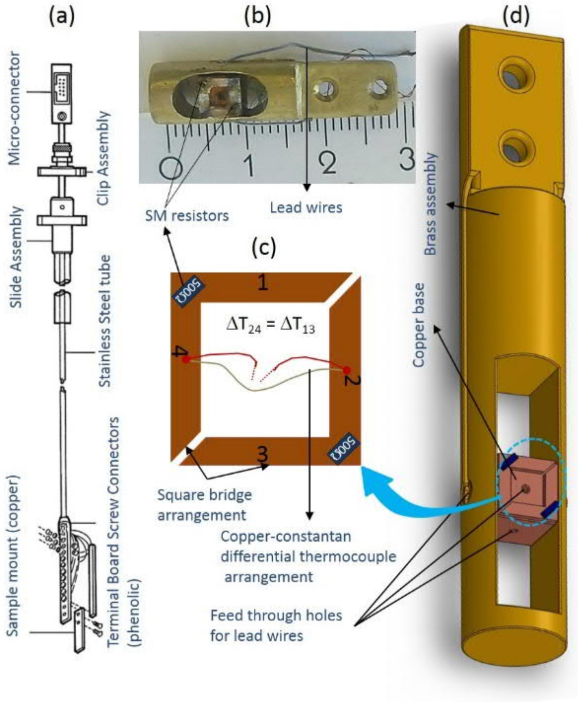

Figure 2. (a) Manual insertion utility probe from quantum design, (b) photo of the actual setup, (c) zoomed image of the square bridge arrangement on copper base, and (d) schematic image of the whole setup.

2.1 Square bridge arrangement and SM resistor positions

The square bridge arrangement is fitted on a cubic copper base of 5x5x5 mm^3 in size fabricated from high-grade copper metal. The system is made electrically insulating by sticking a thin layer of Kapton tape (polyimide film) to avoid any electrical connection between the square copper bridges and the copper base. The two copper bridges are similar and cut diagonally from a square copper strip of 4.5 mm in length, 0.5 mm in thickness and 1.5 mm in width. The bridges are then glued on the cubic copper base with GE 7301varnish as shown in Figure 2(c), to be completed for the sample mounting. Note that the bridges do not touch each other, but there is a gap of about ~0.5 mm at the ends to avoid any direct effect of heating of one bridge on the other.

Two miniature SM resistors of 500 Ω are used to create ΔT along the samples; these are glued using GE varnish at the opposite corners of the square bridges, symmetric from both ends. Placing the SM resistors at the corner positions is important to allow the Seebeck measurement of samples in two equivalent positions, (1,3) and (2,4), with only one differential thermocouple arrangement. As can be understood from Figure 2(c), at a constant base temperature when one of the SM resistors is heated the ΔT between positions (1,3) and (2,4) is equivalent. It should be emphasized that, in several test measurements with or without magnetic fields, no significant difference was observed in Seebeck voltages for samples placed between the two equivalent positions.

The use of SM resistors for creating the ΔT has several advantages such as the fact that they are very inexpensive and can be easily mounted on plane surfaces. For the ΔT measurement across the sample the two differential thermocouple tips are fabricated with high gauge (SWG 44; Standard Wire Gauge) type-T thermocouple wires and soldered in the middle of the sides of the square copper bridges as shown in Figure 2(c). The thinner (high gauge) thermocouple wires ensure low thermal leakages and better thermal anchoring compared to the thicker (low gauge) wires. Both the bridges are again covered with very thin Kapton tape (~6 μm) to avoid any electrical connection between the Seebeck voltage probes, thermocouples, and resistors.

2.2 Differential thermocouple arrangement

The differential arrangement of thermocouples provides great convenience in direct measurement of temperature difference between two points provided the temperature versus voltage characteristics of the thermocouple system is known. In the present setup copper-constantan type-T thermocouple system is used to measure the ΔT across the sample between position (2,4) and/or equivalently (1,3). The use of two separate sensors to measure ΔT has also been reported in literature [29], however, this approach suffers from inherent errors due to subtraction of large numerical values to estimate small values [33]. For the present setup the two differential thermocouple tips are fabricated by welding a copper wire on the two ends of a constantan wire as shown in Figure 3. The open ends of the copper wires are thermally anchored on the brass assembly and connected to the terminal board screw connectors on the MIUP for data acquisition.

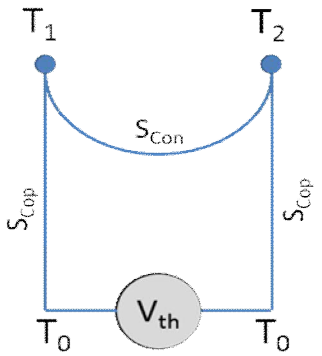

Figure 3. Differential arrangement of thermocouples.

The brass assembly acts as the reference for base temperature for the differential thermocouples at any temperature. The temperature of the brass assembly is noted from the MPMS temperature which remains stable within ±10 mK for the entire measurement. When the SM resistors are powered to create ΔT across the sample, the base temperature may fluctuate in maximum ca. 1–2 degs. at temperatures around 10 K, but no appreciable changes were observed above 50 K. A typical of 10 mA current to SM resistors is sufficient to create a ΔT of 0.5-2.0 K across the sample at different base temperatures. When either of the SM resistors is heated the temperature gradient across the sample can be calculated from the differential thermal voltage of the thermocouple system. The differential thermal voltage (V_{th}) is calculated from the absolute Seebeck coefficients of constantan and copper thermocouple wires, S_{Con} and S_{Cop}, at the base temperature T_0 (see Figure 3) as follows:

$$V_{th} = -\int_{T_0}^{T_1} S_{Cop}\,dT - \int_{T_1}^{T_2} S_{Con}\,dT - \int_{T_2}^{T_0} S_{Cop}\,dT$$

$$= \int_{T_0}^{T_1} S_{Cop}\,dT \quad \int_{T_1}^{T_2} S_{Con}\,dT + \int_{T_0}^{T_1} S_{Cop}\,dT + \int_{T_1}^{T_2} S_{Cop}\,dT$$

$$V_{th} = -\int_{T_1}^{T_2} (S_{Con} - S_{Cop})\,dT$$

When the difference T_2–T_1 is small compared to average temperature $(T_2 + T_1)/2$, then:

$$V_{th} = -(T_2 - T_1) * (S_{Con} - S_{Cop})$$

The temperature versus Seebeck voltage characteristics for the present thermocouple system $(S_{Con} - S_{Cop})$ can be calculated at each base temperature (T_0) using the NIST ITS 90-thermocouple database. Thus, at any base temperature, $\Delta T = (T_2 - T_1)$can be calculated by dividing the measured V_{th} by the estimated $(S_{Con} - S_{Cop})$ at that temperature.

2.3 Measurement of Seebeck voltage

For the measurements of ΔT, ΔV, and the creation of the temperature gradient along the sample via SM resistors (see Figure 4), 8 lead wires of MIUP are used. High resistance wires are used for voltage measurements and low resistance wires for currents to SM resistors. Both the input channels 1 and 2 of Agilent 34420A nanovoltmeter are used to record the ΔV and ΔT, respectively. Advantest R6142 DC current source is used to heat the SM resistors. The diodes arrangement at output of the current source facilitates alternate heating of SM resistors using only one current source for "+" and "–" currents. Reversing the direction of ΔT along the sample and then averaging the ΔV and ΔT cancels the constant voltage contributions, if any, to the measured ΔV and ΔT. All measurement wires are thermally anchored on the cubic copper base and brass assembly that also acts as the isothermal reference junction for thermocouples.

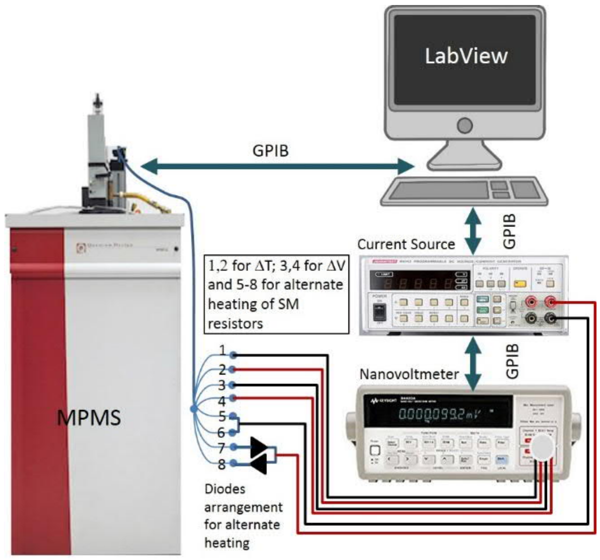

Figure 4. Schematic illustration of the measurement units for data acquisition.

The measurement sample can be mounted equivalently between positions (1,3) and (2,4) as the SM resistors are symmetrically placed w.r.t. either positions. DuPont 4929N silver paste is used to mount the sample on the bridge for good thermal contact between the sample and the bridge; also, it can easily be dissolved in hexyl acetate which acts as thinner for silver paste. The thermocouple tips remain electrically insulated from the sample with the thin Kapton-tape. For the measurements thinner samples would be best to measure the anisotropic effects; however, samples of thickness up to 1 mm can be measured. Samples thicker than 1 mm will be inconvenient during mounting the setup in the MPMS. As one needs to pull the whole setup assembly in the glass tube at the back end of the MIUP before inserting it into the MPMS. The glass tube has the inner diameter of 8 mm and sample might touch the inner wall of the tube. A schematic diagram of the entire measurement unit and data acquisition is shown in Figure 4. The detailed measurement procedure and algorithm of measurement were reported by us in our earlier publication of Seebeck coefficient measurement using a liquid nitrogen cryostat from 77 to 500 K [32].

3. Calibration and testing

Several measurements were performed with various standard samples to calibrate the setup. For the present discussion we focus on the measurements performed on a high-purity (99.99%) thin (500 μm) platinum wire under zero field as well as magnetic fields perpendicular and parallel to temperature gradient as shown in Figure 5. All the measurements were performed with respect to copper lead wires.

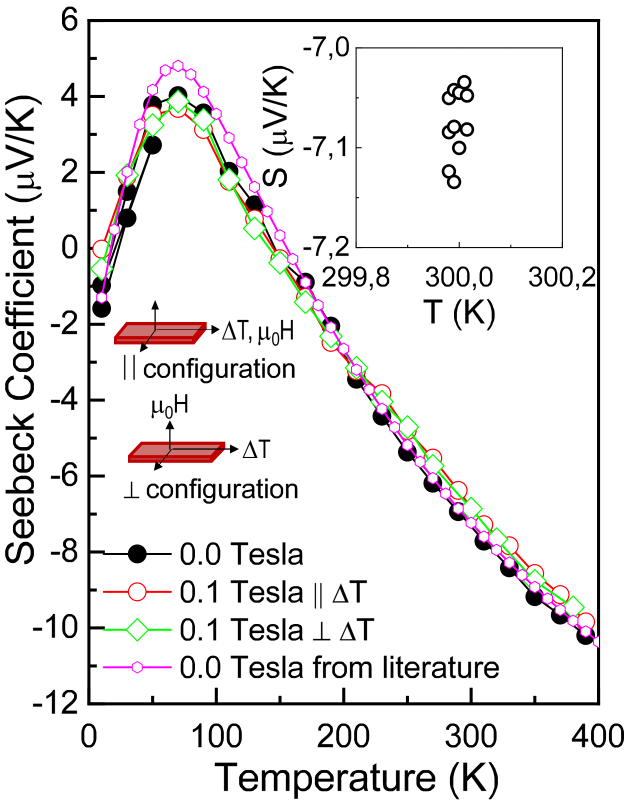

Figure 5. Seebeck coefficient of Pt wire w.r.t. temperature in zero as well as presence of magnetic fields along different directions. Inset shows the measurement accuracy of Seebeck values at a fixed temperature 300 K in zero field condition.

For the reference correction the absolute Seebeck coefficient of copper wire was estimated from the relation for pure Cu wire [34]:

$$S_{Cop} = 0.041T\left[\exp\left(\frac{-T}{93}\right) + 0.123 - \frac{0.442}{1+\left(\frac{T}{172.4}\right)^3}\right] + 0.804$$

The Seebeck coefficient of platinum wire is negative and in good agreement with its simulated values estimated from the relation for pure Pt wire [34]:

$$S_{Pt} = 0.186T\left[\exp\left(\frac{-T}{88}\right) - 0.0786 + \frac{0.43}{1+\left(\frac{T}{84.3}\right)^4}\right] - 2.57$$

Moreover, the estimated value corresponds well to the experimental results [35-38]. As expected, no appreciable effect of magnetic field on the Seebeck coefficient of Pt wire is observed whether the magnetic field is perpendicular or parallel to the temperature gradient. The inset in Figure 5 depicts the maximum fluctuation in Seebeck coefficient measurements for several data points at fixed temperature 300 K and zero magnetic fields. The maximum fluctuations are less than ±0.2 μV/K.

Further to check the directional dependence of Seebeck coefficient on the magnetic field we measured the Seebeck coefficient of $CuCr_2Se_4$ single crystal flakes in the presence of 0.1 Tesla magnetic fields in parallel and perpendicular configurations as displayed in Figure 5. The $CuCr_2Se_4$ single crystal flakes are cubic in symmetry and show preferred orientation along 111 direction based on X-ray diffraction data (not shown here). Directional dependence of Seebeck coefficient on the magnetic field for $CuCr_2Se_4$ was reported by us earlier for bulk powder specimens due to magnon drag effects [17]. The effect of magnetic field can easily be seen as the maximum in Seebeck coefficient due to magnon drag increases and decreases, respectively, for perpendicular and parallel directions w.r.t. zero field value.

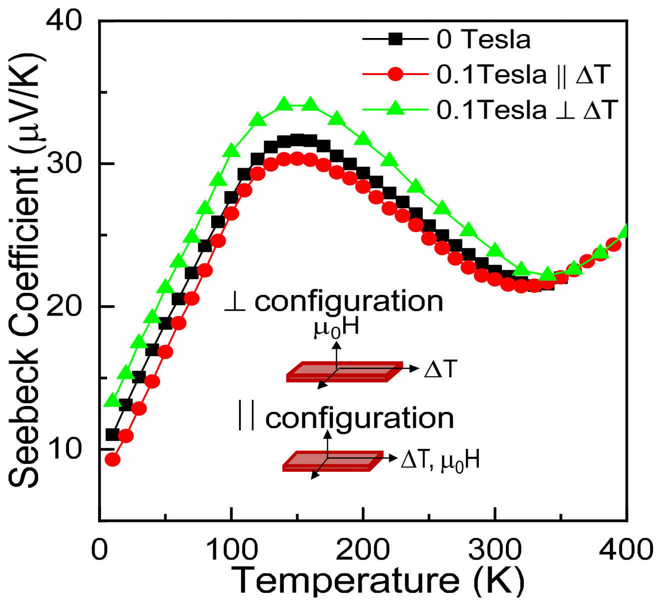

Figure 6. Seebeck coefficient of $CuCr_2Se_4$ single crystal flakes as a function of temperature in presence as well as absence of magnetic fields along different directions.

To evaluate the effect of temperature and magnetic field over the SM resistors we measured (not shown here) the resistance of them for whole temperature range, in presence and the absence of magnetic field both. Resistances show metallic temperature dependence and a maximum change of ±4 Ω is observed in temperature sweep measurements between 10-400 K. No significant change in the resistance is observed due to magnetic field. However, it should be noted that the change of heater resistance should not make any difference to Seebeck coefficient because the Seebeck voltage ΔV depends linearly on the temperature gradient ΔT, and the ratio remains constant.

4. Summary

We have reported a Seebeck coefficient measurement setup in presence or absence of magnetic field in the temperature range from 10 to 400 K. The setup is designed on a MIUP (manual insertion utility probe) for MPMS (magnetic property measurement system; Quantum Design). It is based on the differential technique of Seebeck coefficient measurement and can be utilized to measure the anisotropic Seebeck coefficient in the presence of magnetic field. The direction of magnetic field on the sample can be effectively altered in three directions (along the ΔT, in and out of plane perpendicular to the ΔT) by rotating the set-up along an axis perpendicular to magnetic field. The maximum uncertainty in the measured Seebeck value is less than ±0.2 μV/K, and the accuracy is within 4%.

The setup consists of two miniature SM (surface mount) resistors, placed symmetrically on two square copper bridges, to create the temperature gradient ΔT along the sample. The symmetric mounting of SM resistors allows us to study the effect of magnetic field in three directions: in or out of plane perpendicular to temperature gradient and along the temperature gradient. For the calibration of the setup, Seebeck coefficient of high purity (99.99%) 500 μm thick platinum wire was measured from 10 to 400 K with respect to copper lead wires. To observe the anisotropic effect of magnetic field, Seebeck coefficient of $CuCr_2Se_4$ single crystal flakes was measured in zero field and in the presence of magnetic field. Finally it should also be emphasized that even though the setup was designed for anisotropic Seebeck coefficient measurements, it can also be utilized to measure the anisotropic effects in electrical resistance.

Acknowledgements

We acknowledge the technical support of Mr. Seppo Jääskeläinen in the fabrication of the setup, and the use of the RawMatTERS Finland Infrastructure (RAMI) at Aalto University. This work has received funding from the Academy of Finland (Nos. 292431 and 296299).

References

[1] Cutler M, Mott N F 1969 Observation of Anderson localization in an electron gas *Phys. Rev.* **181** 1336–1340

[2] MacDonald D K C 2006 *Thermoelectricity: An Introduction to the Principles.* Dover publications Inc., Mineola, New York

[3] Zuev Y M, Chang W, Kim P 2009 Thermoelectric and magnetothermoelectric transport measurements of graphene *Phys. Rev. Lett.* **102** 096807-1–4

[4] Gooth J, Schierning G, Felser C, Nielsch K 2018 Quantum materials for thermoelectricity *MRS Bull.* **43** 187–192

[5] He R, Schierning G, Nielsch K 2018 Thermoelectric devices: a review of devices, architectures, and contact optimization *Adv. Mater. Technol.* 1700256-1–17

[6] Xue Y, Zhou X, Zhan T, Jiang B, Guo Q, Fu X, Shimamura K, Xu Y, Mori T, Dai P, Bando Y, Tang C, Golberg D 2018 Densely interconnected porous BN frameworks for multifunctional and isotropically thermoconductive polymer composites *Adv. Func. Mater.* **28** 1801205-1–10

[7] Kosuga A, Nakai K, Matsuzawa M, Fujii Y, Funahashi R, Tachizawa T, Kubota Y, Kifune K 2015 Crystal structure, microstructure, and thermoelectric properties of $GeSb_6Te_{10}$ prepared by spark plasma sintering *J. All. Compd.* **618** 463–468

[8] Tynell T, Terasaki I, Yamauchi H, Karppinen M 2013 Thermoelectric characteristics of (Zn,Al)O/ hydroquinone superlattices *J. Mater. Chem. A* **1** 13619–13624

[9] Niemelä J-P, Karttunen A J, Karppinen M 2015 Inorganic-organic superlattice thin films for thermoelectrics, *J. Mater. Chem. C* **3** 10349–10361

[10] Zhu T, Liu Y, Fu C, Heremans J P, Snyder J G, Zhao X 2017 Compromise and synergy in high-efficiency thermoelectric materials *Adv. Mater.* **29** 1605884

[11] Borup K A, Boor J D, Wang H, Drymiotis F, Gascoin F, Shi X, Chen L, Fedorov M I, Müller E, Iversen B B, Snyder J G 2015 Measuring thermoelectric transport properties of materials *Energy Environ. Sci.* **8** 423–435

[12] Bala M, Gupta S, Srivastava S K, Amrithapandian S, Tripathi T S, Tripathi S K, Dong C L, Chen C L, Avasthi D K, Asokan K 2017 Evolution of nanostructured single-phase $CoSb_3$ thin films by low-energy ion beam induced mixing and their thermoelectric performance *Phys. Chem. Chem. Phys.* **19** 24886–24895

[13] Uchida K, Takahashi S, Harii K, Ieda J, Koshibae W, Ando K, Maekawa S, Saitoh E 2008 Observation of the spin Seebeck effect *Nature* **455** 778–781

[14] Mandal P R, Sarkar T, Higgins J S, Greene R L 2018 Nernst effect in the electron-doped cuprate superconductor $La_{2-x}Ce_xCuO_4$ *Phys. Rev. B* **97** 014522-1–11

[15] Liang T, Lin J, Gibson Q, Gao T, Hirschberger M, Liu M, Cava R J, and Ong N P 2017 Anomalous Nernst effect in the Dirac semimetal Cd_3As_2 *Phys. Rev. Lett.* **118** 136601-1–5

[16] Paglione J, Tanatar M A, Hawthorn D G, Ronning F, Hill R W, Sutherland M, Taillefer L, Petrovic C 2006 Field induced quantum critical point in $CeCoIn_5$ *Phys. Rev. Lett.* **97** 106606-1–4

[17] Tripathi T S, Tewari G C, Rastogi A K 2010 The study of magnon-drag effects in the thermopower of $CuCr_2X_4$ (X = S, Se and Te) *J. Phys.: Conf. Ser.* **200** 032060-1–4

[18] Dresselhaus M S, Chen G, Tang M Y, Yang R G, Lee H, Wang D Z, Ren Z F, Fleurial J-P, Gogna P 2007 New directions for low-dimensional thermoelectric materials *Adv. Mater.* **19** 1043–1053

[19] Wang X, Wang Z M 2013 Nanoscale Thermoelectrics, Springer Science & Business Media, Berlin, Germany

[20] Huang W, Da H, Liang G 2013 Thermoelectric performance of MX_2 (M = Mo, W; X = S, Se) monolayers *J. Appl. Phys*. **113** 104304-1–8

[21] Wickramaratne D, Zahid F, Lake R K 2014 Electronic and thermoelectric properties of few-layer transition metal dichalcogenides *J. Chem. Phys.* **140** 124710-1–13

[22] Chiritescu C, Cahill D G, Nguyen N, Johnson D, Bodapati A, Keblinski P, Zschack P 2007 Ultralow thermal conductivity in disordered, layered WSe_2 crystals *Science* **315** 351–353

[23] Wang J, Xie F, Cao X-H, An S-C, Zhou W-X, Tang L-M, Chen K Q 2017 Excellent thermoelectric properties in monolayer WSe_2 nanoribbons due to ultralow phonon thermal conductivity *Sci. Rep.* **7** 41418-1–8

[24] Wan C, Gu X, Dang F, Itoh T, Wang Y, Sasaki H, Kondo M, Koga K, Yabuki K, Snyder G J, Yang R, Koumoto K 2015 Flexible n-type thermoelectric materials by organic intercalation of layered transition metal dichalcogenide TiS_2 *Nat. Mater.* **14** 622–627

[25] Terasaki I, Sasago Y, Uchinokura K 1997 Large thermoelectric power in $NaCo_2O_4$ single crystals *Phys. Rev. B* **56** R12685(R)

[26] Kushvaha S S, Hofbauer W, Loke Y C, Singh S P, O'Shea S J 2011 Thermoelectric measurements using different tips in atomic force microscopy *J. Appl. Phys.* **109** 084341-1–8

[27] Lyeo H-K, Khajetoorians A A, Shi L, Pipe K P, Ram R J, Shakouri A, Shih C K 2004 Profiling the thermoelectric power of semiconductor junctions with nanometer resolution *Science* **03**(5659) 816–818

[28] Xu W, Shi Y, Hadim H 2010 The fabrication of thermoelectric $La_{0.95}Sr_{0.05}CoO_3$ nanofibers and Seebeck coefficient measurement *Nanotechnol.* **21** 395303-1–4

[29] Mun E, Bud'ko S L, Torikachvili M S, Canfield P C 2010 Experimental setup for the measurement of the thermoelectric power in zero and applied magnetic field *Meas. Sci. Technol.* **21** 055104-1–8

[30] Berglund C N, Beairstro R C 1967 An automatic technique for accurate measurements of Seebeck coefficient *Rev. Sci. Instrum.* **38** 66–68

[31] Martin J, Tritt T, Uher C C 2010 High temperature Seebeck coefficient metrology *J. Appl. Phys.* **108** 121101-1–12

[32] Tripathi T S, Bala M, Asokan K 2014 An experimental setup for the simultaneous measurement of thermoelectric power of two samples from 77 K to 500 K *Rev. Sci. Instrum.* **85** 085115-1–7

[33] Ashok T R, Phillip M, Chong Z, Jeffrey T I, John E B 2012 Measurement of the high-temperature Seebeck coefficient of thin films by means of an epitaxially regrown thermometric reference material *Rev. Sci. Instrum.* **83** 093905-1–5

[34] Rowe D M 2006 Thermoelectrics Handbook: Macro to Nano, CRC Press, Boca Raton, Florida

[35] Cusack N, Kendall P 1958 The absolute scale of thermoelectric power at high temperature *Proc. Phys. Soc*. **72** 898–901

[36] Burkov A T, Heinrich A, Konstantinov P P, Nakama T, Yagasaki K 2001 Experimental set-up for thermopower and resistivity measurements at 100-1300 K *Meas. Sci. Technol.* **12** 264–272

[37] Moore J P, Graves R S 1973 Absolute Seebeck coefficient of platinum from 80 to 340 K and the thermal and electrical conductivities of lead from 80 to 400 K *J. Appl. Phys.* **44** 1174-1178

[38] Guan A, Wang H, Jin H, Chu W, Guo Y, Lu G 2013 An experimental apparatus for simultaneously measuring Seebeck coefficient and electrical resistivity from 100 K to 600 K *Rev. Sci. Instr.* **84** 043903-1-5